



Article

Stabilization of Recycled Concrete Aggregate Using High Calcium Fly Ash Geopolymer as Pavement Base Material

Sermsak Tiyasangthong¹, Piyathida Yoosuk¹, Kitsada Krosoongnern¹, Ratchanon Sakdinakorn¹, Wisitsak Tabyang², Worawit Phojan³ and Cherdasak Suksiripattanapong^{1,*}

¹ Infrastructure and Rail Transportation Technologies Research Unit, Department of Civil Engineering, Faculty of Engineering and Technology, Rajamangala University of Technology Isan, Nakhon Ratchasima 30000, Thailand

² Department of Civil Engineering, Faculty of Engineering, Rajamangala University of Technology Srivijaya, Songkhla 90000, Thailand

³ Department of Civil Engineering, Faculty of Engineering, Northeastern University, Khon Kaen 40000, Thailand

* Correspondence: cherdasak.su@rmuti.ac.th

Abstract: This research investigated high calcium fly ash geopolymer stabilized recycled concrete aggregate (RCA-FAG) as pavement base material. The effect of recycled concrete aggregate (RCA):high calcium fly ash (FA) ratios, sodium silicate (Na₂SiO₃):sodium hydroxide (NaOH) ratio, and curing time on the unconfined compressive strength (UCS) and scanning electron microscope (SEM) properties of RCA-FAG samples were evaluated. The maximum dry unit weight of the RCA-FAG sample was 20.73 kN/m³ at RCA:FA ratio of 80:20 and Na₂SiO₃:NaOH ratio of 60:40. The 7-d UCS of the RCA-FAG samples increased as the FA content and Na₂SiO₃:NaOH ratio increased. The 7-d UCS of the RCA-FAG sample was better than that of the RCA with no FA because FA particles filled in RCA particles, resulting in a dense matrix. The 7-d UCS of RCA-FAG samples passed the 7-d UCS requirement for the low-traffic road. All ingredients met the 7-d UCS requirement for the high-traffic road except the sample with RCA:FA of 100:0 and Na₂SiO₃:NaOH of 50:50 and 60:40. The 7-d SEM images indicated that spherical FA and RCA particles are bonded together, resulting in the dense matrix for all Na₂SiO₃:NaOH ratios. The proposed equation for predicting the UCS of RCA-FAG offered a good coefficient of correlation, which is useful in designing pavement base material from RCA-FAG material.

Keywords: infrastructure construction; recycled concrete aggregate; high calcium fly ash; geopolymer



Citation: Tiyasangthong, S.; Yoosuk, P.; Krosoongnern, K.; Sakdinakorn, R.; Tabyang, W.; Phojan, W.; Suksiripattanapong, C. Stabilization of Recycled Concrete Aggregate Using High Calcium Fly Ash Geopolymer as Pavement Base Material. *Infrastructures* **2022**, *7*, 117. <https://doi.org/10.3390/infrastructures7090117>

Academic Editor: Kevin Paine

Received: 8 August 2022

Accepted: 5 September 2022

Published: 7 September 2022

Publisher's Note: MDPI stays neutral with regard to jurisdictional claims in published maps and institutional affiliations.



Copyright: © 2022 by the authors. Licensee MDPI, Basel, Switzerland. This article is an open access article distributed under the terms and conditions of the Creative Commons Attribution (CC BY) license (<https://creativecommons.org/licenses/by/4.0/>).

1. Introduction

Infrastructure construction tends to increase due to population growth, migration, and urbanization, which leads to growing economies and developing countries. Pavement structure (including a surface course), binder course, base course, subbase, and subgrade, is one of the transportation infrastructures that has used a massive number of natural resources and generated a large quantity of construction and demolition (C&D) materials [1,2]. Every year, 30 billion tons of C&D materials are generated worldwide [3]. The United States [4], Australia [5], China [6], and Thailand [7] produced C&D materials of 584, 19.6, 1130, and 1.1 million tons, respectively. Several researchers have explored the use of recycled concrete aggregate (RCA) in pavement construction [8–17]. They reported that RCA needs to be improved by a binder (cement, lime, and fly ash) due to low physical properties (high water absorption and porosity) and engineering properties (low strengths) [11–13]. Nonetheless, cement manufacturing emits huge quantities of carbon dioxide (CO₂) into the atmosphere [18–21].

The alternative binder material, geopolymer, has lower CO₂ emissions than cement [22,23]. For example, Tabyang et al. [15] investigated the CO₂ emissions of municipal solid waste

incineration fly ash (MSWI FA) geopolymer and cement stabilized RCA. The cement stabilized RCA was a 22.60% higher CO₂ emission than MSWI FA geopolymer stabilized RCA. However, the geopolymerization products need a temperature range between 40 °C and 80 °C in order to be promoted [24], resulting in high energy consumption [25,26]. Therefore, several researchers have reported the enhancement of properties of geopolymer material using high calcium, such as calcium carbide residue [27], slag [28], and high calcium fly ash (FA) [29]. Nuaklong et al. [30] reported that the setting time of the FA-based geopolymer sample exhibited a high rate of hardening, resulting from the rapid calcium silicates hydrate (CSH) formation [31]. In addition, high calcium in geopolymer materials created calcium aluminate silicate hydrate (CASH) products, which was a lower porosity than the sodium aluminate silicate hydrate (NASH) products [32]. Yoosuk et al. [23] examined the compressive strength of FA geopolymer mortar. They reported that the maximum compressive strength of FA geopolymer mortar was 20.94 MPa at the Na₂SiO₃:NaOH ratio of 1 and NaOH concentration of 8 M. Recently, Chindaprasirt et al. [33] investigated the effect of different binders (FA, ordinary Portland cement, basalt fiber, and silica fume) on the compressive strength of geopolymer mortar. They concluded that 10% of ordinary Portland cement offered maximum compressive strength.

Several research studies have already been conducted on geopolymer-stabilized RCA. For example, Mohammadinia et al. [8] investigated the unconfined compressive strength of fly ash and cement kiln dust stabilized RCA. The highest UCS of the sample was found at FA:cement kiln dust ratio of 50:50. Arulrajah et al. [9] examined RCA stabilized by calcium carbide residue (CCR) and class F FA geopolymer. The UCS of CCR-FA geopolymer stabilized RCA was higher than that of FA geopolymer stabilized RCA because Ca from FA and RCA was not enough to react with silica [34]. Furthermore, FA-rice husk ash (RHA)geopolymer improved RCA was investigated by Poltue et al. [35]. The higher RHA resulted in a decrease in UCS because high Si gels from RHA hinder water evaporation. The 60RHA:40FA ratio and 50NaOH:50Na₂SiO₃ ratio of FA-RHA geopolymer stabilized RCA provided the optimum ingredient. Based on the strength requirement given by the national road authority of Thailand [36,37], Tabyang et al. [15] reported the optimum liquid content, 90RCA:10MSWI FA ratio, and 60Na₂SiO₃:40NaOH of RCA-MSWI FA geopolymer samples passed the 7-d UCS requirement for the high traffic road.

Although several studies have been undertaken to evaluate the mechanical behavior of class F FA geopolymer stabilized RCA, the mechanical properties of the RCA-high calcium fly ash geopolymer under ambient room temperature have never been investigated. This study evaluated the properties of recycled concrete aggregate using high calcium fly ash geopolymer (RCA-FAG) as pavement base material. The studied influence factors included RCA:FA ratios, Na₂SiO₃:NaOH ratio and curing time. The unconfined compressive strength (UCS) and scanning electron microscope (SEM) tests were used to examine the strength development and microstructure in the RCA-FAG samples. The proposed equation for predicting the UCS of RCA-FAG should be very useful for designing pavement base material.

2. Materials and Methods

2.1. Materials

The RCA was sourced from the Rajamangala University of Technology Isan in Nakhon Ratchasima, Thailand. Based on ASTM C128-15 [38], the specific gravity was 2.61. Figure 1 illustrates the grain size of the RCA based on the Department of highway standard. The RCA had a median grain size of 10 mm and was categorized as well-graded gravel (GW) by the Unified Soil Classification System. The modified Proctor compaction evaluated by ASTM D1557 [39] of RCA yielded the maximum dry unit weight of 19.95 kN/m³ and the optimal water content of 9.8%.

Fly ash (FA) was collected from the Mae Moh power plant in Thailand. The specific gravity of FA was 2.46. The chemical properties according to ASTM E1621 [40] are indicated in Table 1. The CaO content was 31.41% and SiO₂ + Al₂O₃ + Fe₂O₃ was 63.41%. It was

classified as class C following the standard ASTM C618-19 [41]. The median grain size was 0.02 mm as indicated in Figure 1.

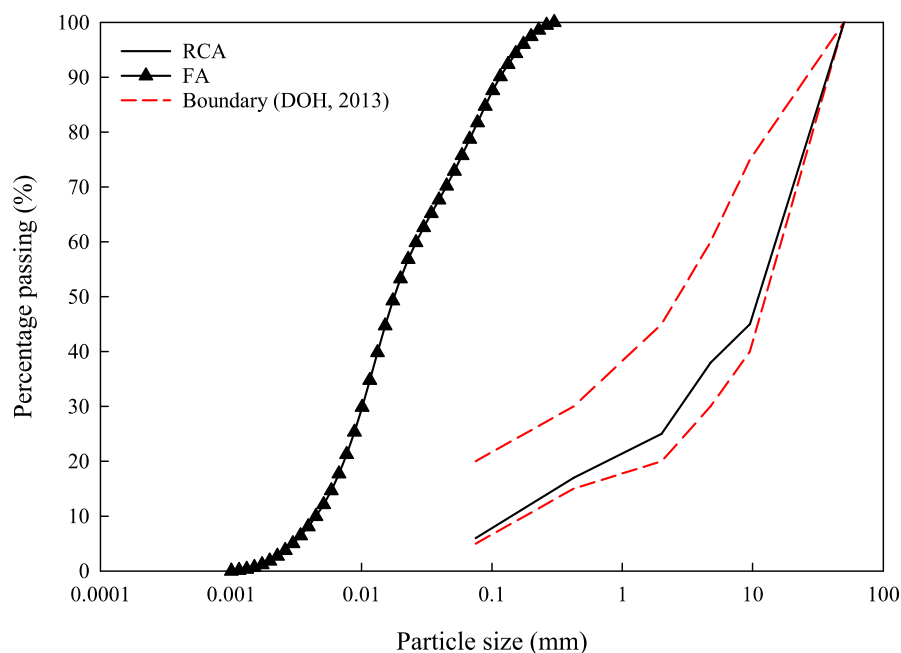


Figure 1. The particle size of RCA and FA.

Table 1. Chemical composition of FA.

Chemical Compositions	FA (%)
SiO ₂	45.44
Al ₂ O ₃	10.53
Fe ₂ O ₃	7.44
CaO	31.41
SO ₃	2.02
K ₂ O	2.20
LOI	0.96

Sodium silicate (Na₂SiO₃) and sodium hydroxide (NaOH) were used as liquid alkaline activators (L). The Na₂SiO₃ with 9% Na₂O and 30% SiO₂ by weight and 98% purity of NaOH were used.

2.2. Sample Preparation and Testing

RCA, FA, and L (Na₂SiO₃ and NaOH) were used to prepare RCA-FAG samples. In this study, the ratios of RCA:FA were 100:0, 90:10, 80:20, and 70:30, while the ratios of Na₂SiO₃:NaOH were 80:20, 60:40, 70:30, and 50:50. The NaOH concentration of 8 molars was fixed. Mix proportions of RCA-FAG samples are shown in Table 2.

Table 2. Mix proportions of RCA-FAG samples.

Item	Compaction Test	UCS Test
RCA:FA	100:0, 90:10, 80:20, 70:30	100:0, 90:10, 80:20, 70:30
L content (% by weight of total)	Between 5–14	Optimum liquid content
Na ₂ SiO ₃ :NaOH ratios	80:20, 60:40, 70:30, 50:50	80:20, 60:40, 70:30, 50:50
NaOH concentration (molars)	8	8
Curing time (days)	-	7, 14, 28, 60

RCA and FA were mixed for 5 min in order to prepare a sample for this investigation. Following the addition of *L*, the sample was mixed for 10 min to guarantee its homogeneity. Modified Proctor compaction was used to compact the RCA-FAG samples. Different *L* contents were used to establish the optimal liquid content (OLC) for each RCA:FA ratio. After acquiring the OLC, the specimens were made with a diameter of 101.6 mm and a height of 116.4 mm. The samples were then plastic-wrapped. After 7, 14, 28, and 60 days of curing at room temperature (27–30 °C), the unconfined compressive strength (UCS) according to ASTM D4318-00 [42] of samples was measured by using a universal testing machine (UTM). Small RCA-FAG samples were collected from the center and their scanning electron microscope (SEM) analysis was assessed [43,44].

3. Results and Discussion

3.1. Compaction of RCA-FAG

Figure 2 indicates the relationship between FA content and maximum dry unit weight of RCA-FAG samples at different RCA:FA and Na₂SiO₃:NaOH ratios. The optimum liquid content of RCA-FAG samples was 8.46–11.75% for all RCA:FA and Na₂SiO₃:NaOH ratios. Poltue et al., 2019 [35] reported a similar result when investigating compaction curves of FA geopolymer stabilized RCA. The RCA-FAG sample had the maximum dry unit weight of 20.73 kN/m³ at an RCA:FA ratio of 80:20 and Na₂SiO₃:NaOH ratio of 60:40. In contrast, the minimum dry unit weight of an RCA-FAG sample was an RCA:FA ratio of 100:0 and Na₂SiO₃:NaOH ratio of 70:30, which was 19.26 kN/m³. When the FA content increased, the maximum dry unit weight increased. For example, maximum dry unit weight values of RCA-FAG samples with Na₂SiO₃:NaOH ratio of 60:40 were 19.58, 20.43, 20.73, and 20.35 kN/m³ for RCA:FA ratios of 100:0, 90:10, 80:20, and 70:30, respectively. For FA contents more than 20%, the maximum dry unit weight of RCA-FAG samples dropped due to FA’s lower specific gravity [18,19].

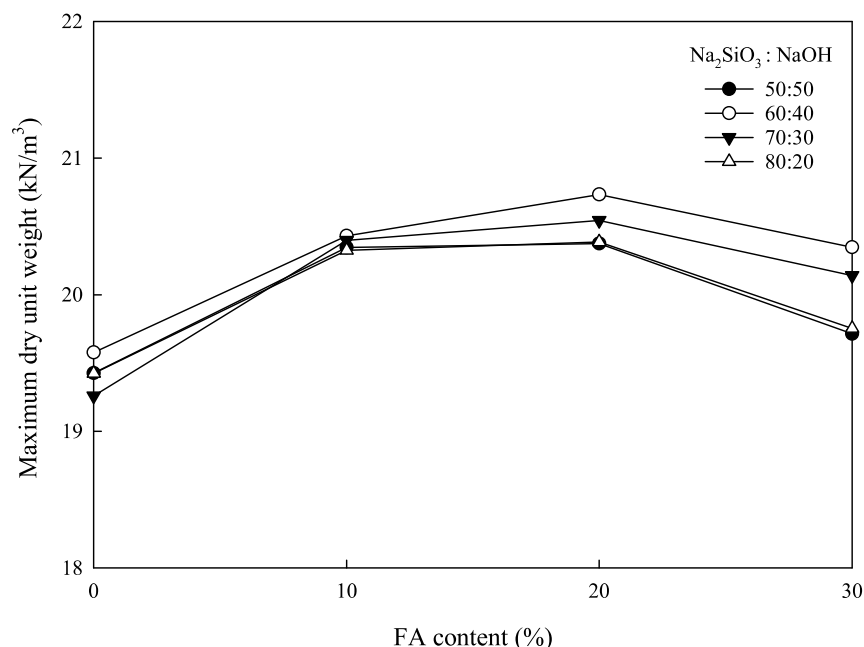


Figure 2. The relationship between FA content and maximum dry unit weight of RCA-FAG samples.

3.2. Unconfined Compressive Strength of RCA-FAG

Figure 3 indicates the 7-d UCS of RCA-FAG samples at different RCA:FA and Na₂SiO₃:NaOH ratios. The 7-d UCS of RCA-FAG samples increased as FA content increased. For example, the 7-d UCS of RCA-FAG samples at Na₂SiO₃:NaOH ratio of 70:30 were 2.50, 9.55, 11.92, and 15.37 MPa for FA content of 0, 10, 20, and 30, respectively. This is because silica and alumina from FA can react with calcium, which results in pozzolan

and geopolymerization products [33]. The 7-d UCS of the RCA-FAG sample was better than that of the RCA with no FA because FA particles filled in RCA particles, resulting in a dense matrix [15].

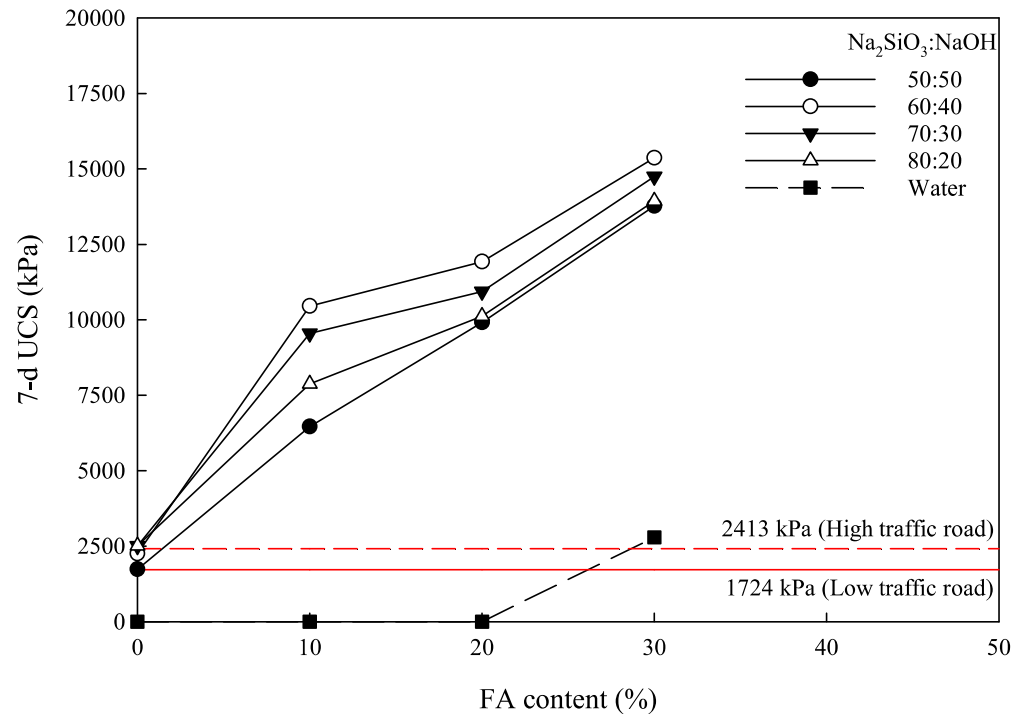


Figure 3. The 7-d UCS of RCA-FAG samples.

The effect of the Na₂SiO₃:NaOH ratio on 7-d UCS of RCA-FAG samples is shown in Figure 3. The 7-d UCS of RCA-FAG samples increased with the Na₂SiO₃:NaOH ratio because calcium silicate hydrate (CSH) and sodium aluminosilicate gels [8,26] resulted from a silicate reaction with calcium from FA and RCA. Until the Na₂SiO₃:NaOH ratio was 60:40, the 7-d UCS of RCA-FAG samples decreased as the Na₂SiO₃:NaOH ratio increased. A similar result was reported by Tabyang et al. [15], who concluded that the addition of Na₂SiO₃ caused UCS reduction because the packing effect resulted from the high viscosity of Na₂SiO₃. The RCA:FA ratio of 70:30 and Na₂SiO₃:NaOH ratio of 70:30 of RCA-FAG sample exhibited the maximum 7-d UCS of 15.37 MPa.

Figure 3 indicates red lines as the 7-d UCS requirement for specified low traffic and high traffic roads of pavement base material [36,37]. The 7-d UCS of RCA-FAG samples passed the 7-d UCS requirement for the low-traffic road. For the high-traffic road, all ingredients met the 7-d UCS requirement except the sample with RCA:FA of 100:0 and Na₂SiO₃:NaOH of 50:50 and 60:40.

3.3. UCS Development in RCA-FAG

Figure 4 indicates the UCS development in RCA-FAG samples at different RCA:FA ratios and Na₂SiO₃:NaOH ratios. For RCA-FAG samples, the UCS increased with an increase in curing time. For example, the UCS of RCA-FAG samples with RCA:FA ratios of 70:30 and Na₂SiO₃:NaOH ratios of 60:40 were 15.37, 20.32, 22.41, and 23.91 MPa for curing times of 7, 14, 28, and 60 days, respectively. The increased UCS because the coexistence of calcium silicate hydrate (CSH) and geopolymerization products resulted from NaOH continually leached silica and alumina from FA [15]. On the other hand, for samples with no FA, the UCS of the sample was slightly increased with an increase in curing time due to insufficient silica and alumina from FA for geopolymerization reaction [34].

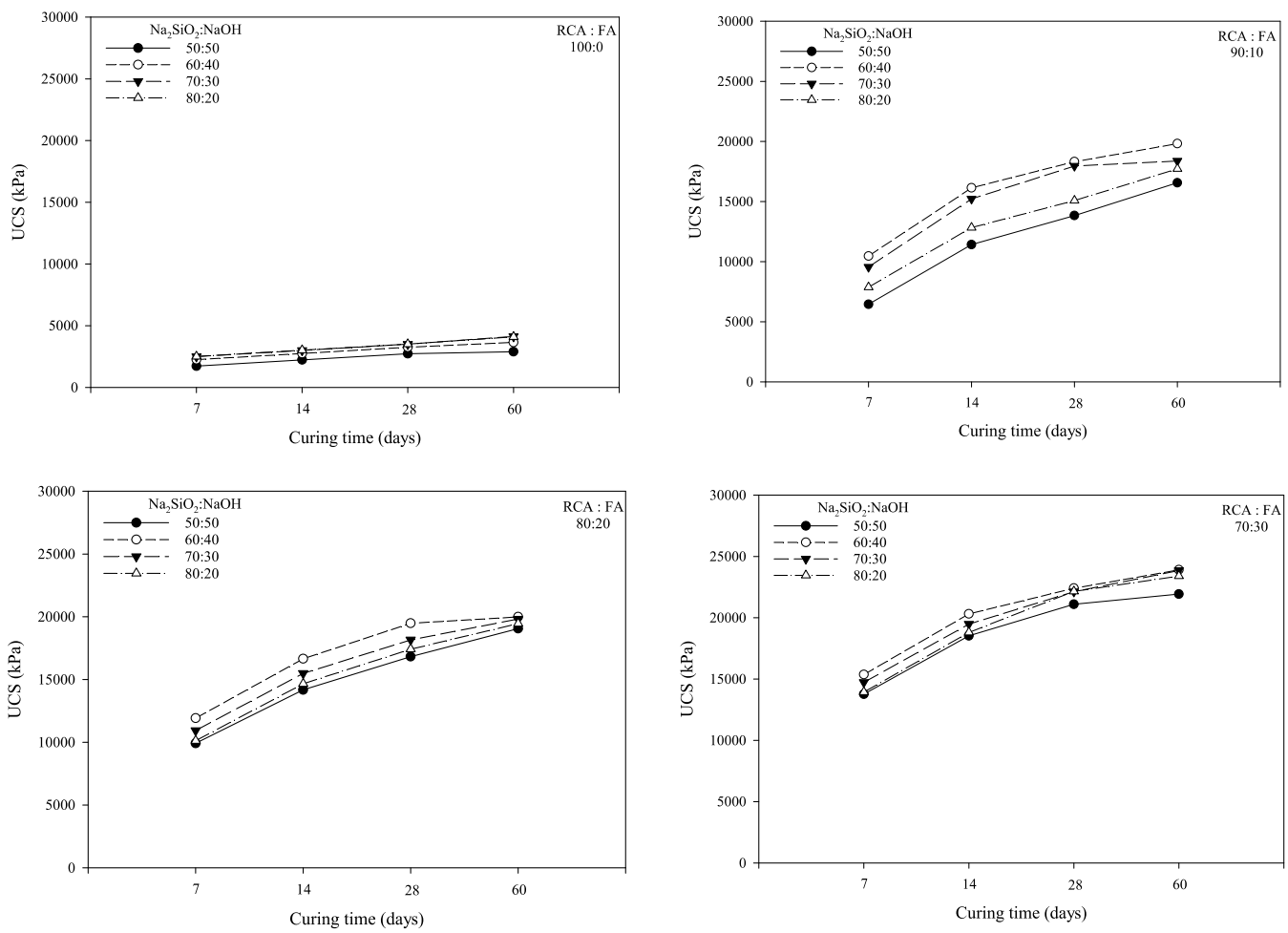


Figure 4. The UCS development in RCA-FAG samples.

Figure 5 shows the relationship between UCS/28-d UCS and the curing time of RCA-FAG samples. It can be seen that the UCS development in RCA-FAG samples can be normalized by 28-d UCS. The correlation of normalized UCS/28-d UCS of RCA-FAG samples at different RCA:FA ratios and Na₂SiO₃:NaOH ratios was expressed by a logarithmic function as follows:

$$UCS/28\text{-d UCS} = 0.219 + \ln(d)0.237 \quad \text{for } 7 < d < 60 \text{ days} \quad (1)$$

with a coefficient of correlation of 0.89. The proposed equation is useful for predicting the UCS of RCA-FAG samples when 28-d UCS is known.

3.4. SEM Images of RCA-FAG

Figure 6 illustrates 7-d SEM images of RCA-FAG samples at RCA:FA = 80:20 and Na₂SiO₃:NaOH = 50:50, 60:40, 70:30, and 80:20. It can be observed that spherical FA and RCA particles are bonded together, resulting in the dense matrix for all Na₂SiO₃:NaOH ratios. At optimum Na₂SiO₃:NaOH of 60:40, the products with etched holes were found on the FA surface, indicating the complete degree of a chemical reaction [25] and associating with the highest 7-d UCS of 15.37 MPa. For Na₂SiO₃:NaOH of 70:30 and 80:20, the high Na₂SiO₃ content resulted in voids due to the high viscosity of Na₂SiO₃ and some unreacted FA particles were observed, which were 7-d UCS of 14.74 and 13.94 MPa, respectively.

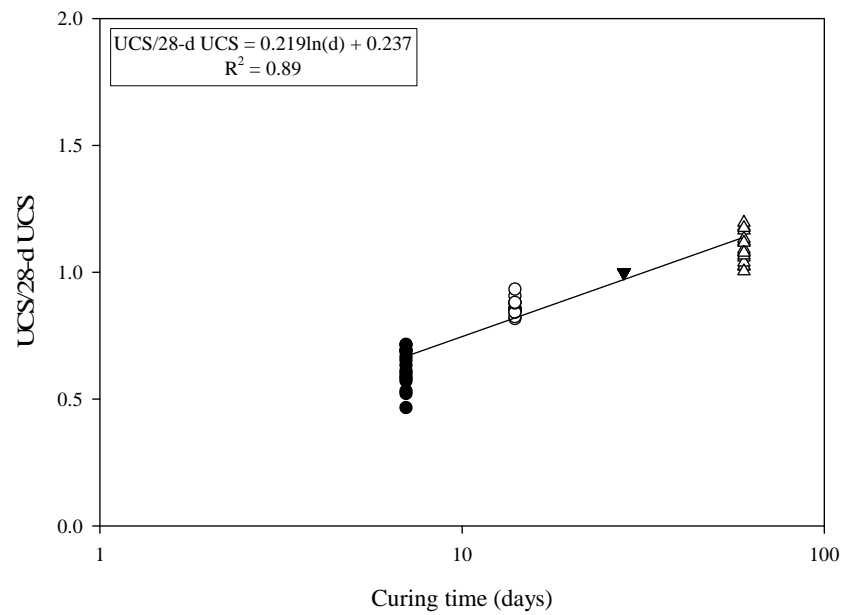


Figure 5. The relationship between UCS/28-d UCS and curing time of RCA-FAG samples.

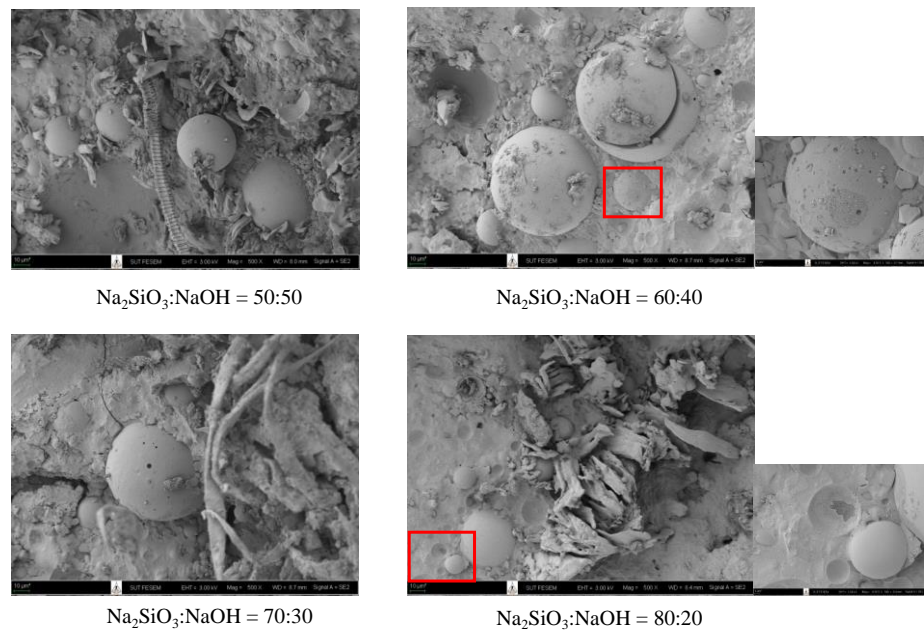


Figure 6. 7-d SEM images of RCA-FAG samples at RCA:FA = 80:20 and Na₂SiO₃:NaOH = 50:50, 60:40, 70:30, and 80:20.

4. Conclusions

The effect of RCA:FA ratios, Na₂SiO₃:NaOH ratio, and curing time on the UCS of RCA-FAG samples can be concluded as follows:

1. The optimum liquid content of RCA-FAG samples was 8.46–11.75% for all RCA:FA and Na₂SiO₃:NaOH ratios. The maximum dry unit weight of the RCA-FAG sample was 20.73 kN/m³ at RCA:FA ratio of 80:20 and Na₂SiO₃:NaOH ratio of 60:40.

2. The 7-d UCS of RCA-FAG samples increased as FA content raised because FA silica and alumina from FA can react with calcium, resulting in pozzolan and geopolymerization products. The 7-d UCS of RCA-FAG sample was better than that of the RCA with no FA because FA particles filled in RCA particles, resulting in a dense matrix.

3. The 7-d UCS of RCA-FAG samples increased with the $\text{Na}_2\text{SiO}_3\text{:NaOH}$ ratio because calcium silicate hydrate (CSH) and sodium aluminosilicate gels resulted from a silicate reaction with calcium from FA and RCA.

4. The 7-d UCS of RCA-FAG samples passed the 7-d UCS requirement for the low-traffic road. All ingredients met the 7-d UCS requirement for the high-traffic road, except the sample with RCA:FA of 100:0 and $\text{Na}_2\text{SiO}_3\text{:NaOH}$ of 50:50 and 60:40.

5. The UCS of RCA-FAG samples increased as curing time increased because the coexistence of calcium silicate hydrate (CSH) and geopolymerization products resulted from NaOH continually leached silica and alumina from FA. The proposed equation for predicting UCS of RCA-FAG offered a good coefficient of correlation, which is useful in designing pavement base material from RCA-FAG material.

6. The 7-d SEM images indicated that spherical FA and RCA particles are bonded together, resulting in the dense matrix for all $\text{Na}_2\text{SiO}_3\text{:NaOH}$ ratios. Recommendations for further research on the RCA-FAG include the evaluation of flexural strength and indirect tensile strength tests, the effect of water absorption of RCA, and durability against wetting–drying cycles.

Author Contributions: Conceptualization, C.S. and S.T.; methodology, P.Y., S.T. and R.S.; investigation, C.S., S.T. and K.K.; resources, S.T. and C.S.; writing—original draft preparation, C.S.; writing—review and editing, S.T., P.Y., K.K., R.S., W.P. and W.T.; supervision, S.T.; project administration, S.T.; funding acquisition, S.T. All authors have read and agreed to the published version of the manuscript.

Funding: This research project is supported by Thailand Science Research and Innovation (TSRI), contract No. FRB650059/NMA/19.

Institutional Review Board Statement: Not applicable.

Informed Consent Statement: Not applicable.

Data Availability Statement: Not applicable.

Acknowledgments: The first and seventh authors acknowledge the financial support from Rajamangala University of Technology Isan.

Conflicts of Interest: The authors declare no conflict of interest.

References

1. Verian, K.P.; Ashraf, W.; Cao, Y. Properties of recycled concrete aggregate and their influence in new concrete production. *Resour. Conserv. Recycl.* **2018**, *133*, 30–49. [CrossRef]
2. Rahman, S.S.; Khattak, M.J. Roller compacted geopolymer concrete using recycled concrete aggregate. *Constr. Build. Mater.* **2021**, *283*, 122624. [CrossRef]
3. Pawluczuk, E.; Kalinowska-Wichrowska, K.; Jiménez, J.R.; Fernández-Rodríguez, J.M.; Suescum-Morales, D. Geopolymer concrete with treated recycled aggregates: Macro and microstructural behavior. *J. Build. Eng.* **2021**, *44*, 103317. [CrossRef]
4. United States Environmental Protection Agency. Advancing Sustainable Materials Management. 2015 Fact Sheet; 2018; p. 22. Available online: <https://www.epa.gov/facts-and-figures-about-materials-waste-and-recycling/advancing-sustainable-materials-management> (accessed on 7 August 2022).
5. Pickin, J.; Randell, P. *Australian National Waste Report 2017*; Department of the Environment and Energy, 2016; p. 82. Available online: <https://www.dceew.gov.au/sites/default/files/documents/national-waste-report-2016.pdf> (accessed on 7 August 2022).
6. Lu, W.S.; Webster, C.; Peng, Y.; Chen, X.; Zhang, X.L. Estimating and calibrating the amount of building-related construction and demolition waste in urban China. *Int. J. Constr. Manag.* **2017**, *17*, 13–24. [CrossRef]
7. Kofoworola, O.F.; Gheewala, S.H. Environmental life cycle assessment of a commercial office building in Thailand. *Int. J. Life Cycle Assess.* **2008**, *13*, 498–511. [CrossRef]
8. Mohammadinia, A.; Arulrajah, A.; D'Amico, A.; Horpibulsuk, S. Alkali-activation of fly ash and cement kiln dust mixtures for stabilization of demolition aggregates. *Constr. Build. Mater.* **2018**, *186*, 71–78. [CrossRef]
9. Arulrajah, A.; Mohammadinia, A.; Phummiphan, I.; Horpibulsuk, S.; Samingthong, W. Stabilization of Recycled Demolition Aggregates by Geopolymers comprising Calcium Carbide Residue, Fly Ash and Slag precursors. *Constr. Build. Mater.* **2016**, *114*, 864–873. [CrossRef]
10. Ding, Y.; Li, H.; Zhang, H.; Li, S.; Zhang, X.; Hua, S.; Zhao, J.; Tong, Y. Shrinkage and durability of waste brick and recycled concrete aggregate stabilized by cement and fly ash. *Materials* **2022**, *15*, 3684. [CrossRef]

11. Mohammadinia, A.; Arulrajah, A.; Sanjayan, J.; Disfani, M.M.; Bo, M.W.; Darmawan, S. Stabilization of demolition materials for pavement base/subbase applications using fly ash and slag geopolymers: Laboratory investigation. *J. Mater. Civ. Eng.* **2016**, *28*, 04016033. [[CrossRef](#)]
12. Kavussi, A.; Hassani, A.; Kazemian, F.; Taghipoor, M. Laboratory evaluation of treated recycled concrete aggregate in asphalt mixtures. *Int. J. Pavement Res. Technol.* **2019**, *12*, 26–32. [[CrossRef](#)]
13. Xing, W.; Tam, V.W.Y.; Le, K.N.; Hao, J.L.; Wang, J. Life cycle assessment of recycled aggregate concrete on its environmental impacts: A critical review. *Constr. Build. Mater.* **2022**, *317*, 125950. [[CrossRef](#)]
14. Sereewatthanawut, I.; Prasittisopin, L. Environmental evaluation of pavement system incorporating recycled concrete aggregate. *Int. J. Pavement Res. Technol.* **2020**, *13*, 455–465. [[CrossRef](#)]
15. Tabyang, W.; Suksiripattanapong, C.; Phetchuay, C.; Laksanakit, C.; Chusilp, N. Evaluation of municipal solid waste incineration fly ash based geopolymer for stabilised recycled concrete aggregate as road material. *Road Mater. Pavement Des.* **2021**, *23*, 2178–2189. [[CrossRef](#)]
16. Arulrajah, A.; Disfani, M.M.; Horpibulsuk, S.; Suksiripattanapong, C.; Prongmanee, N. Physical properties and shear strength responses of recycled construction and demolition materials in unbound pavement base/subbase applications. *Constr. Build. Mater.* **2014**, *58*, 245–257. [[CrossRef](#)]
17. Kou, S.C.; Poon, C.S. Long-term mechanical and durability properties of recycled aggregate concrete prepared with the incorporation of fly ash. *Cem. Concrete. Compos.* **2013**, *37*, 12–19. [[CrossRef](#)]
18. Suksiripattanapong, C.; Horpibulsuk, S.; Phetchuay, C.; Suebsuk, J.; Phoo-ngernkham, T.; Arulrajah, A. Water treatment sludge–calcium carbide residue geopolymers as nonbearing masonry units. *J. Mater. Civ. Eng.* **2017**, *29*, 04017095. [[CrossRef](#)]
19. Suksiripattanapong, C.; Phetprapai, T.; Singsang, W.; Phetchuay, C.; Thumrongvut, J.; Tabyang, W. Utilization of recycled plastic waste in fiber reinforced concrete for eco-friendly footpath and pavement applications. *Sustainability* **2022**, *14*, 6839. [[CrossRef](#)]
20. Suksiripattanapong, C.; Jenpiyapong, K.; Tiyasangthong, S.; Krittacom, B.; Phetchuay, C.; Tabyang, W. Mechanical and thermal properties of lateritic soil mixed with cement and polymers as a non-bearing masonry unit. *Case Stud. Constr. Mater.* **2022**, *16*, e00962. [[CrossRef](#)]
21. Song, H.; Ahmad, A.; Farooq, F.; Ostrowski, K.A.; Maślak, M.; Czarnecki, S.; Aslam, F. Predicting the compressive strength of concrete with fly ash admixture using machine learning algorithms. *Constr. Build. Mater.* **2021**, *308*, 125021. [[CrossRef](#)]
22. Tabyang, W.; Suksiripattanapong, C.; Wonglakorn, N.; Laksanakit, C.; Chusilp, N. Utilization of municipal solid waste incineration fly ash for non-bearing masonry units containing coconut fiber. *J. Nat. Fibers* **2022**, 1–14. [[CrossRef](#)]
23. Yoosuk, P.; Suksiripattanapong, C.; Sukontasukkul, P.; Chindaprasirt, P. Properties of polypropylene fiber reinforced cellular lightweight high calcium fly ash geopolymer Mortar. *Case Stud. Constr. Mater.* **2021**, *15*, e00730. [[CrossRef](#)]
24. Suksiripattanapong, C.; Sakdinakorn, R.; Tiyasangthong, S.; Wonglakorn, N.; Phetchuay, C.; Tabyang, W. Properties of soft Bangkok clay stabilized with cement and fly ash geopolymer for deep mixing application. *Case Stud. Constr. Mater.* **2022**, *16*, e01081. [[CrossRef](#)]
25. Sukmak, P.; Horpibulsuk, S.; Shen, S.L.; Chindaprasirt, P.; Suksiripattanapong, C. Factors influencing strength development in clay-fly ash geopolymer. *Constr. Build. Mater.* **2013**, *40*, 1125–1136. [[CrossRef](#)]
26. Azad, N.M.; Samarakoon, S.S.M. Utilization of industrial by-products/waste to manufacture geopolymer cement/concrete. *Sustainability* **2021**, *13*, 873. [[CrossRef](#)]
27. Chindaprasirt, P.; Jaturapitakkul, C.; Chalee, W.; Rattanasak, U. Comparative study on the characteristics of fly ash and bottom ash geopolymers. *Waste Manag.* **2009**, *29*, 539–543. [[CrossRef](#)]
28. Phetchuay, C.; Horpibulsuk, S.; Suksiripattanapong, C.; Chinkulkijniwat, A.; Arulrajah, A.; Disfani, M.M. Calcium carbide residue: Alkaline activator for clay-fly ash geopolymer. *Constr. Build. Mater.* **2014**, *69*, 285–294. [[CrossRef](#)]
29. Arulrajah, A.; Kua, T.A.; Suksiripattanapong, C.; Horpibulsuk, S. Stiffness and strength properties of spent coffee grounds-recycled glass geopolymers. *Road Mater. Pavement Des.* **2017**, *20*, 623–638. [[CrossRef](#)]
30. Nuaklong, P.; Wongsu, A.; Sata, V.; Boonserm, K.; Sanjayan, J.; Chindaprasirt, P. Properties of high-calcium and low-calcium fly ash combination geopolymer mortar containing recycled aggregate. *Heliyon* **2019**, *5*, e02513. [[CrossRef](#)]
31. Chindaprasirt, P.; De Silva, P.; Sagoe-Crentsil, K.; Hanjitsuwan, S. Effect of SiO₂ and Al₂O₃ on the setting and hardening of high calcium fly ash-based geopolymer systems. *J. Mater. Sci.* **2012**, *47*, 4876–4883. [[CrossRef](#)]
32. Ismail, I.; Bernal, S.A.; Provis, J.L.; San Nicolas, R.; Brice, D.G.; Kilcullen, A.R.; Hamdan, S.; van Deventer, J.S. Influence of fly ash on the water and chloride permeability of alkali-activated slag mortars and concretes. *Constr. Build. Mater.* **2013**, *48*, 1187–1201. [[CrossRef](#)]
33. Chindaprasirt, P.; Sriopas, B.; Phosri, P.; Yoddumrong, P.; Anantakarn, K.; Kroehong, W. Hybrid high calcium fly ash alkali-activated repair material for concrete exposed to sulfate environment. *J. Build. Eng.* **2022**, *45*, 103590. [[CrossRef](#)]
34. Phetchuay, C.; Horpibulsuk, S.; Arulrajah, A.; Suksiripattanapong, C.; Udomchai, A. Development in soft marine clay stabilized by fly ash and calcium carbide residue based geopolymer. *Appl. Clay Sci.* **2016**, *127–128*, 134–142. [[CrossRef](#)]
35. Poltue, T.; Suddeepong, A.; Horpibulsuk, S.; Samingthong, W.; Arulrajah, A.; Rashid, A.S.A. Strength development of recycled concrete aggregate stabilized with fly ash-rice husk ash based geopolymer as pavement base material. *Road Mater. Pavement Des.* **2019**, *21*, 2344–2355. [[CrossRef](#)]
36. *DH-S 203/2556*; Standard for Cement Modified Crushed Rock Base. Department of Highways (DOH): Bangkok, Thailand, 2013.
37. *SDR 244-2556*; Standard for Soil Cement Base. Department of Rural Roads (DRR): Bangkok, Thailand, 2013.

38. *C128-15*; Standard Test Method for Relative Density (Specific Gravity) and Absorption of Fine Aggregate. ASTM: West Conshohocken, PA, USA, 2015.
39. *D1557-12*; Standard Test Methods for Laboratory Compaction Characteristics of Soil Using Modified Effort (56,000 ft-lbf/ft³ (2700 kN-m/m³)). ASTM: West Conshohocken, PA, USA, 2021.
40. *E1621*; Standard Guide for Elemental Analysis by Wavelength Dispersive X-Ray Fluorescence Spectrometry. Annual Book of ASTM Standard. Vol.03.05. ASTM: West Conshohocken, PA, USA, 2013.
41. *C618-19*; Standard Specification for Coal Fly Ash and Raw or Calcined Natural Pozzolan for Use in Concrete. ASTM: West Conshohocken, PA, USA, 2019.
42. *C1633*; Standard Test Methods for Compressive Strength of Molded Soil-Cement Cylinders. ASTM: West Conshohocken, PA, USA, 2000.
43. Suksiripattanapong, C.; Horpibulsuk, S.; Boongrasan, S.; Udomchai, A.; Chinkulkijniwat, A.; Arulrajah, A. Unit weight, strength and microstructure of a water treatment sludge–fly ash lightweight cellular geopolymer. *Constr. Build. Mater.* **2015**, *94*, 807–816. [[CrossRef](#)]
44. Suksiripattanapong, C.; Srijumpa, T.; Horpibulsuk, S.; Sukmak, P.; Arulrajah, A.; Du, Y.J. Compressive strengths of water treatment sludge–fly ash geopolymer at various compression energies. *Low. Technol. Int.* **2015**, *17*, 147–156. [[CrossRef](#)]